# In-situ observation and modelling of solidification and fluid flow on GTAW process

Alexis Chiocca, Fabien Soulié, Frédéric Deschaux-Beaume, Cyril Bordreuil

# In-situ observation and modelling of solidification and fluid flow on GTAW process

**A Chiocca, F Soulié, F Deschaux-Beaume and C Bordreuil**

LMGC - UMR 5508, Université Montpellier 2, CC048 Place Eugène Bataillon 34095 Montpellier Cedex 5, France

E-mail: alexis.chiocca@univ-montp2.fr

**Abstract.**

An experimental setup is presented in order to obtain experimental data during solidification of a static weld pool after arc extinction with a GTAW process. Several devices have been set up to extract three kinds of measurements: *(i)* solidification front velocity *(ii)* fluid flow velocity at the vicinity of the front *(iii)* temperature field in the solid part. A high-speed camera is used to film the interface during welding at microscopic level and an infra-red in order to take the temperature field around the weld pool in the solid part. After processing and calibration of the videos, the experimental results are compared to theoritical results founded on an adapted model from the KGT [1] and from the one of Gandin et al. [2]. All the tests are done thin plate of Cu-30wt.%Ni.

## 1. Introduction

The microstructure of welded joints mainly determines their mechanical properties. The weld bead microstructure results from the solidification process occurring in the weld pool at the solid/liquid interface. This process of solidification includes mechanisms that are driven by heat and fluid flow. The understanding of solidification mechanisms in relation with weld pool behaviour is then a key point to analyse microstructure formation and to control joint strength.

Compared to the common case of solidification such as casting, welding processes induce high thermal gradients and high solutal gradients at the solid/liquid interface and the front velocity is much faster. Due to these solidification conditions, columnar and equiaxed dendritic microstructures are broadly observed. The characteristic length of the weld pool is around 10mm. In the weld pool, fluid flow and heat transfer can be complex and can vary from point to point along the interface [3]. Depending on the position on the solid/liquid interface, the thermal gradient and the solidification speed change. At the trailing edge, the solidification speed is maximal and the thermal gradient is minimal but at the fusion line, it is the opposite. To understand the microstructural evolution along the interface, information from two scales are necessary: *(i)* macroscopic fields around the interface and *(ii)* microscopic observations. Macroscopic fields (temperature gradient, for example) gives driven force for the solidification. On in-situ observations, Zhao et al. [4] proves that the fluid flows have complex shapes that can influence solidification. Microscopic observations tells us the behaviour of the interface (stability and/or fragmentation). Delapp et al. [5] based on microscopic observations showed that fluid flow could produce fluctuation of the front speed giving ripples on the weld bead.

**Table 1.** Parameter used for the analytical model.

| Parameters | Values |
|---|---|
| Liquidus slope, $m$ $(K/wt.\%Ni)$ | 1.40 |
| Partition coefficient, $k$ | 3.89 |
| Nominal alloy composition $C_0$ $(wt.\%Ni)$ | 30 |
| Liquid density, $\rho$ $(g/cm^3)$[8] | 8.1 |
| Gibbs-Thomson coefficient, $\Gamma$ $(K.m)$[2] | 1.96e-7 |
| Stability constant, $\sigma*$[2] | 0.0253 |
| Dynamic viscosity, $\mu$ $(Pa.s)$[9] | 3.1e-3 |
| Liquidus temperature, $T_l$ $(K)$[8] | 1520 |
| Diffusion coefficient $D_l$ $(m^2/s)$[9] | 1e-9 |
| Solidification range $\Delta T_r$ $(K)$[10] | 1472-1520 |

Modelling dendritic growth under weld solidification conditions is still a major issue. Different works introduced important phenomena observed during solidification. Hunziker et al. [6] gives, for the case of welding, an exponential relation between the solidification speed and the total undercooling. Gandin et al. [2] have simulated a dendritic growth with fluid flow showing the interactions between the growth velocity and the fluid flow ahead the interface.

The present work wants to develop a solidification model in welding conditions with the help of different experiments. Experiments are done on Cu30wt.%Ni plate and the front velocity, the fluid flow velocity and the thermal field are analysed under different thermal conditions. Then the comparison is done with the model which is adapted from two different models [2, 6].

## 2. In situ Observations

In this part, experimental setup is described with the two scale devices to investigate solidification under welding conditions. One purpose is to compare microstructure evolution with different solidification conditions induced by different process parameters. The main process parameters are the intensity of welding and the down-slope. The intensity has a direct control on the power input and the down-slope allow the solidification to be slower by decreasing the intensity before the end of welding with a negative slope. In order to estimate the kinetic of solidification, front velocity, the fluid flow velocity and the thermal fields will be measured in-situ.

Details of the experimental setup and errors made in the measurement can be found in an other article [7].

### *2.1. Material*

For an efficient comparison with the theoritical models, the simple binary alloy Cu30Ni has been chosen. This alloy is composed of 70% of copper and 30% of nickel and its phase diagram has only a solid solution in the solid part. The physical parameters useful for the model are listed on table 1. The partition coefficient, the diffusion coefficient and the liquidus slope are supposed constant. The liquid density is taken at the liquidus temperature.

### *2.2. Experimental setup*

The experimental setup design is illustrated on figure 1. The observations are done on a static weld pool after or during the arc extinction. The weld pool generated by a GTAW torch is

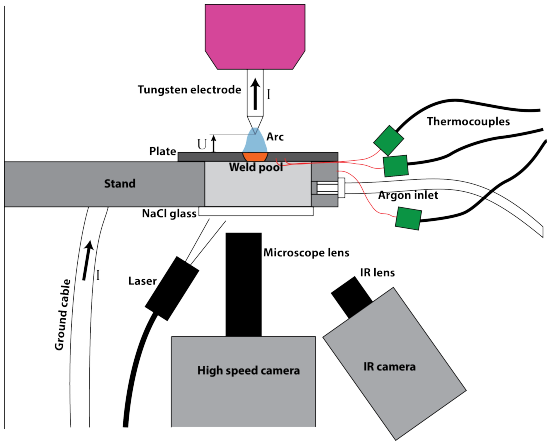


**Figure 1.** Drawing of the set-up showing the different measurements done around the plate.

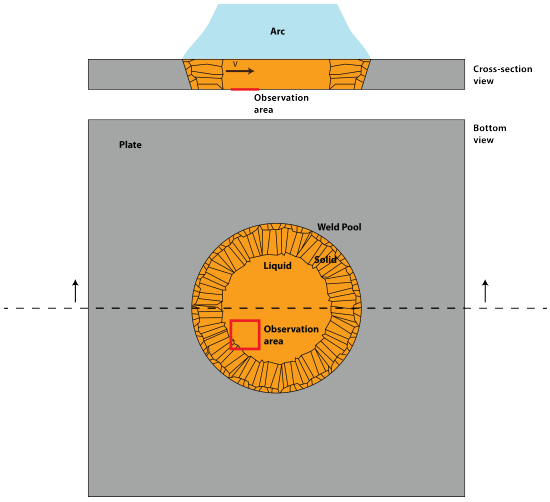


**Figure 2.** Geometrical description of the observed system, at the top a cross-section view and at the bottom a bottom view.

full-penetrated to allow the observation on the back side. On this side, The liquid metal is protected from oxidation by a chamber full of argon. The coupon is 1.6 mm thick and 70 mm of diameter.

Observations of the weld pool for solidification front and fluid flow measurements are obtained thanks to an high speed camera. This camera is placed under the plate and observe the area represented by a square on figure 2. The observation area is lighted up by a LASER in order to insure the segmentation of the liquid and solid phase. The back side of the plate is filmed with the IR camera and two thermocouples are placed below the plate for the calibration of the temperature field. The observation area represent the whole weld pool and a large solid part.

### *2.3. Field measurements*

*2.3.1. Thermal fields* IR camera gives access to temperatures in the solid phase and near the interface on the back surface, after a calibration step with the thermocouples.

The solid part temperature of the sample along a the dashed line on figure 3 is plotted on figure 4. The temperature increases from the edge to the centre of the sample. Due to the calibration procedure, the measured temperature is only available in the solid phase. Nevertheless, the temperature gradient in the solid phase can be approximated. With this setup configuration, the gradients measured are about $2 * 10^5$ $K/m$ and the temperatures at the interface are about 1300 $K$ (Fig. 3 and 4).

*2.3.2. Velocities fields* Two kind of velocities are extracted from the high speed films: the velocities of the solidification front and the velocities of the fluid flow. The velocities of the solidification front are obtained by detecting contours of solidification front in images. The field of velocities in the liquid are computed by Particle Image Velocimetry (PIV) processing [11]. Velocities of particles at the vicinity of the front are estimated around 50 $mm/s$ (Fig. 5 and 6) and front speed are between 1.5 $mm/s$ and 4 $mm/s$ (Fig. 7 and 8) depending on the adjustments of the power source.

Fluid flow curves (Fig. 6) show a peak at the vicinity of the front. The projection of the velocity of the fluid particle is high when it goes out the front and decreases while approaching the weld pool centre. Only few eddies are observed on videos telling us that the flow is mainly

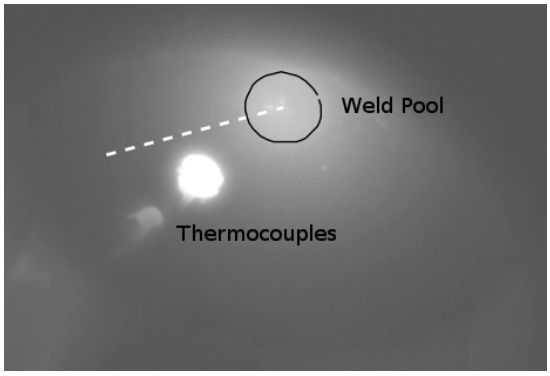


**Figure 3.** Thermal Field under the plate. The plain contour ——circle the weld pool.

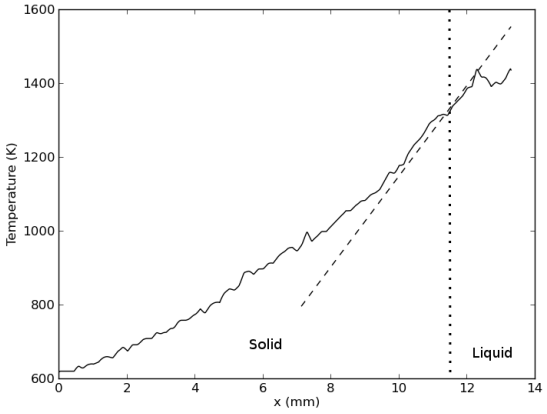


**Figure 4.** The ——curve correspond to temperature along the dashed line - - - -on figure 3. The dashed line - - - -is the temperature gradient at the interface. The approximative limit between solid and liquid is represented by the dotted line .....

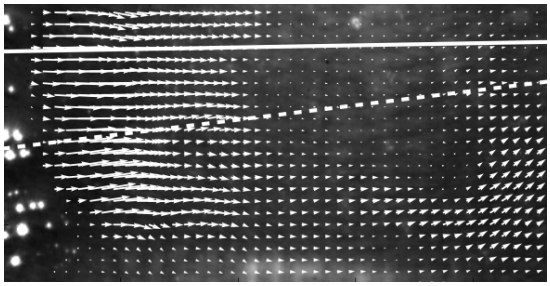

**Figure 5.** Velocity field ahead the front. On the left the dendrite tips growing from the left to the right and on the left the liquid pool.

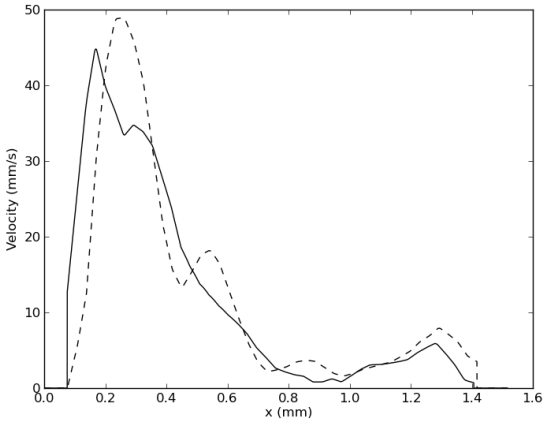


**Figure 6.** Evolution of the velocity vectors from the left to the right along the straight lines on figure 5.

laminar. For the back side, a vortex is observed from the interface to the center of the weld pool. Fluid velocity are more important at the extinction of the arc and then tends to decrease.

The decreasing of the radius of the weld pool (Fig. 8) is almost linear with a decrease of the slope at the end of the curve. Irregularity all along the curve might be caused by oscillation of the weld pool.

*2.4. Observations*

A complete observation test is illustrated on figures 3, 5 and 7. For this test the intensity applied on the electrode is 70 A during 5.5 seconds without down-slope. After extracting and processing data, the solidification speed is 3.43 $mm/s$ (Fig. 8) and the velocity of the fluid flow at the vicinity of the interface is 39 $mm/s$ (Fig. 6). The field of temperature allow us to estimate the

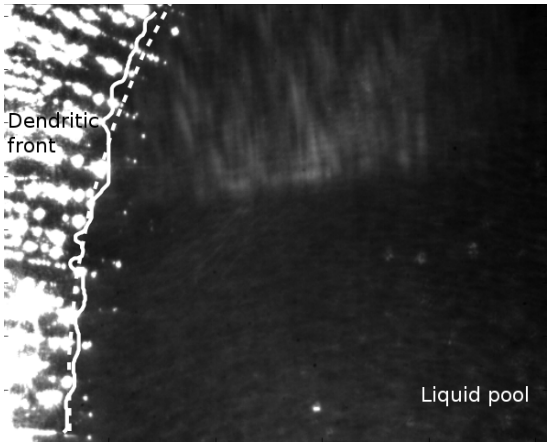


**Figure 7.** Contour detection of the front with in plain line ——the raw contour and in dashed line - - - -the estimated circle.

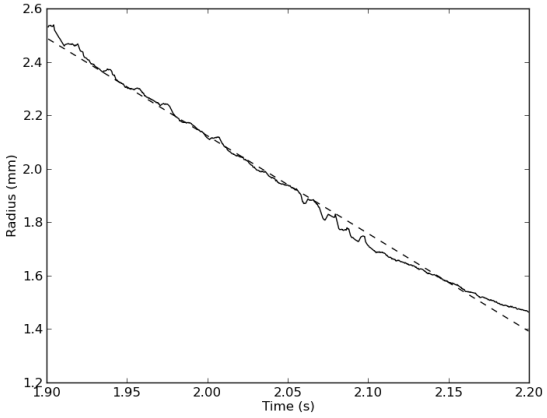


**Figure 8.** In plain line ——the decreasing of the radius of the weld pool across time and in dashed line - - - -the mean slope.

gradient near the interface at $1.82 * 10^5$ $K/m$ and the total undercooling at 191 $K$ (Fig. 4). The undercooling is equal to the difference between the temperature at the interface and the liquidus temperature.

During high speed imaging, small particles are ejected from the interface. The videos tell us that the solidification is mainly columnar and that at the very end some equiaxed grains seems to be observed. All the dendrite tips are submerged during growth. The tip grows below the liquid surface, the dendrite is then visible when the primary branches grow, becoming fatter and joining with its neighbour dendrites.

With measurements, dimensionless numbers can be estimated in order to appreciate the heat and mass transfer in this configuration. In particular, the Péclet numbers show the dominance of convection over diffusion $P_v = \frac{R*v}{D_l}$ and $P_u = \frac{R*u}{D_l}$ with $v$ the solidification speed, $R$ the radius of the dendrite tip and $u = u_{piv} - v$ the velocity of the liquid with respect to the front. These Péclet numbers are respectively estimated at $10^{-1}$ and $10^0$ in order of magnitude, demonstrating that the liquid is well homogenized. The value of the Reynolds number $Re = \frac{\rho u L}{\mu}$ with the experimental velocity is estimated at 1300 confirming the laminar state.

## 3. Welding solidification modeling

It exists a lot of theoretical models on solidification. The variations in the models depend on the conditions of solidification. For example, with slow or rapid solidification. In the case of slow solidification or low Péclet number [12] assumptions can accelerate computations of the model. For welding solidification, the conditions taken for this study are the one found in the KGT model [1]. Kurz et al. have developed a model for rapid solidification with assumptions that can be applied to welding. This model results in two equations with two unknowns:

$$\Delta T = mC_0 \left(1 - \frac{1}{1-(1-k)\Omega}\right) + \frac{2\Gamma}{R} \qquad R = 2\pi\sqrt{\frac{2\Gamma}{mG_c\xi - G}} \tag{1}$$

with $R$ the radius of the dendrite tip, $\xi$ a factor present in the model [1] and $\Omega = Iv()$ the supersaturation equal to the Ivantsov function.

Even if it is suitable for welding, it doesn't take into account the fluid flows. It is only a diffusive model.

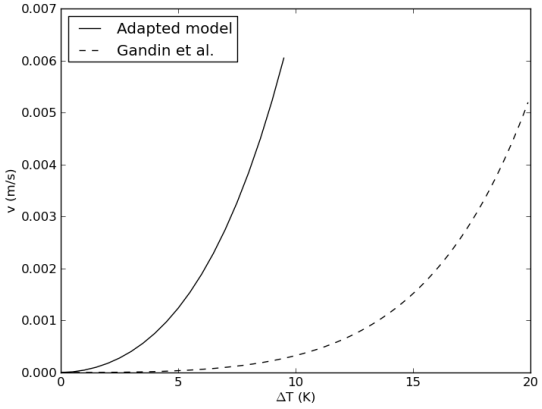


**Figure 9.** Solidification speed with respect to the undercooling.

*3.1. Fluid Velocities*

To implement the fluid flow without using a fully numerical model, one solution is to add a boundary layer $\delta$ ahead the front. It is the solution presented in the article of Gandin et al. [2]. It takes into account the intensity and the direction of the flow by changing the thickness of the layer. Changes are made on the supersaturation:

$$\Omega = P_v exp(P_v)(E_1(P_v) - E_1(P_v(1 + \frac{2\delta}{R}))) \qquad \frac{\delta}{R} = \frac{2}{ARe_{2r}^{B} Sc^{C} sin(\theta/2)} \tag{2}$$

$$E_1(P_v) = \int_{P_v}^{\infty} \frac{exp(-\tau)}{\tau} d\tau \tag{3}$$

with $A$, $B$ and $C$ parameters defined in the article of Gandin et al.[2], $Re$ number of Reynolds and $Sc$ number of Shmidt. However this model, as it is described, is made for low Péclet numbers corresponding to slow solidification.

*3.2. Welding growth*

To take into account high thermal gradients and velocities measured during the experiment, a model is developed. The system to solve is the same one as in equation 1 but the definition of the supersaturation is the one of equation 2. This model shows an exponential relation between the undercooling and the front velocity (Fig. 9). Fluid flow velocity has the strongest influence when it is in the opposite direction of the front growth. But when it is in the same direction, the influence on solidification is weakest and is found null as it is shown in the study of Gandin et al. [2]. In this model, the temperature gradient has no influence on front velocity but a big influence on the stability limit of the planar front. As the gradient increase, the stability limit velocity increases too [1].

## 4. Results and discussions

The models presented previously show relations between intensity and direction of the fluid flow, velocity of the front velocity and thermal parameters. In this section, the purpose is to know if the results coming from the models can be observed experimentally. Different tests are summarized on table 2.

**Table 2.** Results on four tests.

| Test number | Intensity | Down-Slope | $v$ | $u_{piv}$ | $G$ | $\Delta T$ |
|---|---|---|---|---|---|---|
| 1 | 70 A | 0 s | 3.46 mm/s | 39 mm/s | 182.4 K/mm | 191 K |
| 2 | 80 A | 0 s | 3.03 mm/s | 49 mm/s | 184.6 K/mm | 185 K |
| 3 | 90 A | 0 s | 2.90 mm/s | 50 mm/s | 187.9 K/mm | 215 K |
| 4 | 90 A | 2 s | 1.38 mm/s | 50 mm/s | 123.8 K/mm | 226 K |

*4.1. Macroscopic results*

An increase of power input (70 to 90A) leads to larger and hotter weld pool. This can explain the two main differences in the tests : a lower front velocity for 90A and lower fluid velocity for 70A. With higher temperature in the weld pool, it is expected that the front needs to transform more energy to change phase. With higher temperature on the arc surface due to more energetic plasma, the gradient in temperature can be more important leading to higher Marangoni forces inducing higher fluid velocities. The undercooling at the interface, corresponding to the difference between liquidus temperature and the temperature measured at the interface, does not seem to be influenced by the power input of the welding process. Looking at the energy increasing from test 1 to test 4, the undercooling values between test 1 and test 4 have not big variations.

According to the model, the solidification front velocity increase with the level of undercooling at the interface. Between the different test, the same level of undercooling gives different value of solidification speed. With the experimental values applied on the adapted model (Fig. 9), the undercooling found vary between 5 K and 8 K. It is very few compared to the experimental results about 200 K. The values might be wrong because the limit between liquid and solid is blur. The temperatures measured at the interface are underestimated because it is not the temperature of dendrite tip. The dendrites tip might be submerged in the liquid while the measurement is done at the surface, corresponding to a point before the tip where the dendrite has already cooled.

*4.2. Interface behaviour*

At the microscopic level, several variations have to be highlighted. The direction of solidification and the direction of the fluid flow are mainly in the same direction. In the presented model, the fluid flow has in that case no influence on dendritic growth velocity.

From a test to an other, the morphology is dendritic columnar in the window of observation of the high speed camera. If the observation area is placed on the centre of the weld pool, at the end of the solidification, grains which do not come from the front grow inside the liquid bulk. These grains are either equiaxed grains that have nucleated in the bulk or columnar grains coming from the upper side of the plate. The first assumption could be qualitatively explained. At the end of the solidification, the gradient can be lower, the solidification speed accelerate and impurities driven by the flow might be blocked in the centre. If the top of the weld is solidified at first, columnar grains can nucleate and grow downward until the bottom of the weld.

The dendrite spacing measured on all the tests do not show great variations over the dendrites velocity. The spacing between dendrites is more sensitive to the temperature gradient. The changes of spacing between the different measurements have been found coherent with the law of David et al. [13]: $d = a(G^2 v)^{-0.25}$

*4.3. Growth modeling during solidification*

During the solidifcation after arc extinction, it is found that the undercooling keep a quasi constant value while the gradient decrease. These results are coherent with the theory. A constant undercooling verify a constant value of velocity according to the model. The decreasing of the gradient show the flattening of the temperature field and may cause the growth of the supposed equiaxed grains in the centre. It has already been found that discrepancy are observed for fluid flow direction in the range of $[\frac{7\pi}{4}; \frac{\pi}{4}]$ [2]. The model presented in this case is finally found not pertinent for the direction of fluid flow. However the fluid flow does not seems to have an influence on front velocity speed. For three equal velocities of fluid, the front velocities are different.

## 5. Conclusion

Experimental results have been presented on solidification of a binary alloy (Cu-wt.%30Ni) processed by GTAW. Several welding conditions have been carried out to vary solidification conditions. Assumption have been made to explain the results and to compare them to the modelling data. A lot of data, that was not measured yet, are determined in this study: the solidification front velocity, the fluid flow velocity and the thermal field.

The macroscopic observations explain the solidification behaviour. The velocities are driven by the thermal conditions, the undercooling only plays a role for the position of the dendrite front between solidus and liquidus.

The lack of accuracy of the thermal measurements are the main problem of the difficulty to set experiments against modelling. It is not possible to measure the temperatures of dendrite tip inside the liquid. A way of improvement could be a prediction of the dendrite temperature tip with the available informations on the gradient and the temperatures.

## References


[1] Kurz W, Giovanola B and Trivedi R 1986 *Acta Metallurgica* **34** 823–830
[2] Gandin C A, Guillemot G, Appolaire B and Niane N 2003 *Materials Science and Engineering: A* **342** 44–50
[3] Kou S 2003 *Welding Metallurgy* (John Wiley & Sons, Inc.)
[4] Zhao C X, Van Steijn V, Richardson I M, Saldi Z and Kleijn C R 2009 *ASM Proceedings of the International Conference: Trends in Welding Research* (Pine Mountain, GA, United states) pp 201–210
[5] DeLapp D, Cook G, Strauss A and Hofmeister W 2005 *Proceedings of the 7th Internatioanl Conference on Trends in Welding Research* 97–102
[6] Hunziker O, Dye D and Reed R 2000 *Acta Materialia* **48** 4191–4201
[7] Chiocca A, Bordreuil C, Deschaux-Beaume F and Soulié F *Science and Technology of Welding and Joining*
[8] Brillo J and Egry I 2003 *International journal of thermophysics* **24** 1155–1170
[9] Chakraborty N 2009 *Applied Thermal Engineering* **29** 3618–3631
[10] Hüpf T, Cagran C, Kaschnitz E and Pottlacher G 2010 *International Journal of Thermophysics* **31** 966–974
[11] Prasad A K 2000 *Curr. Sci. (India)* **79** 51–60
[12] Dantzig J A and Rappaz M 2009 *Solidification* 1st ed (EPFL Press)
[13] David S and Vitek J 1989 *International Materials Reviews* **34** 213